Structure and Properties Enhancement in Poly(phenylene sulfide) Melt Spun Fibers. III. Effect of Two Zone Drawing and Annealing

Prabhakar Gulgunje, Gajanan Bhat, Joseph Spruiell

Department of Materials Science and Engineering, The University of Tennessee, Knoxville, Tennessee

Received 23 February 2011; accepted 24 August 2011
DOI 10.1002/app.35519
Published online 17 January 2012 in Wiley Online Library (wileyonlinelibrary.com).

ABSTRACT: This article discusses the enhancement of structure and morphology of PPS fibers by annealing and two zone draw-annealing. Also investigated is the comparison between fiber morphology and properties achieved by single zone draw-annealing vis-à-vis extended annealing and two zone draw-annealing. Annealing of undrawn as-spun fibers yields tenacities around 4.5 gpd (grams/denier). It is shown that when compared with one zone drawing, two zone drawing improves PPS fibers' drawability and enhances the tensile properties significantly. Fibers spun from high molecular weight PPS resins, when drawn and annealed under optimum processing conditions during two zone draw-annealing, possess tenacities around 6 gpd. A model for the fiber structure is proposed based on the morphological studies. © 2012 Wiley Periodicals, Inc. J Appl Polym Sci 125: 1693–1700, 2012

Key words: fibers; structure–property relations; high performance polymers; extrusion; thermoplastics

INTRODUCTION

Detailed investigation of the influence of melt spinning variables and of one zone draw-annealing on structure–properties enhancement in PPS melt spun fibers was reported in our earlier publications.[1,2] It has been reported by several investigators that increasing the number of draw zones and thereby achieving the possible drawability in stages helps in improving the fiber tensile properties further.[3,4] Suzuki et al.[5] reported improvements in fiber properties by multizone drawing and annealing of industrially produced as-spun PPS fibers. Steam assisted multizone drawing and annealing of melt spun fibers produced from Fortron® PPS led to fiber tenacity close to 60 cN/tex (6 gpd—grams per denier) with elongation to break around 18%.[6] Young's modulus achieved was around 400 to 450 cN/tex at 0.5 to 2% extension. However, there is lack of detailed investigation of structure–properties comparison between one zone draw-annealed versus extended annealed and two zone-draw annealed PPS fibers. Findings of these comparisons are reported in this article.

Correspondence to: G. Bhat (gbhat@utk.edu).

Contract grant sponsors: Ticona Polymers (a business of Celanese Chemicals), and Center for Materials Processing at The University of Tennessee, Knoxville.

MATERIALS AND EXPERIMENTAL METHODS

Details of polymers and experimental methods used to manufacture as-spun fibers were provided in our earlier publications.[1,2] Three variations of proprietary Fortron® linear PPS resins in the pellets form were supplied by Ticona Polymers, a business of Celanese Chemicals. The sample codes are 1P, 2P, and 3P. The melt flow indices of these samples are 190, 150, and 61, respectively. Therefore, the order of MW is 1P < 2P < 3P. Each of these polymers were melt spun using pilot scale melt spinning facility comprising of Fourne single screw extruder. The 12 holes spinneret with 0.8-mm diameter capillary was used to produce multifilament as-spun yarns. The methods relevant to the present investigation and not discussed in prior publications are discussed below in detail. Due to their repetitive nature throughout the discussion, a few terms are abbreviated and their explanations are as follows: DA stands for draw annealing, EA stands for extended annealing, D-A-EA stands for draw-annealing-extended annealing, 1ZD-A stands for one zone draw-annealing, and 2ZD-A stands for two zone draw-annealing.

Annealing

To investigate the influence of annealing without drawing on fiber properties enhancement, as-spun fibers spun at low throughput and highest take-up speed, possessing very little drawability were selected

for this study. The fibers were annealed at 170°C by continuously passing through a 10-cm long tubular heater at a speed of 15 mpm (meters per minute).

To investigate the influence of additional annealing at elevated temperatures, yarns drawn in a single zone at a draw temperature of 95°C and annealed using the 10-cm long heater at 150°C as discussed in detail in our earlier publication,[2] were further passed through 1-m long heater that was placed after the third draw roll pair. The long heater was maintained at 190°C. Experiments were also conducted at higher annealing temperatures of 210°C. Threadline continuity could not be obtained and fibers were sticking to the heater surface at annealing temperature of 210°C. Experiments performed using short annealing heater followed by long annealing heater are referred to as EA in following discussions. The process was operated at a speed of 15 ± 2 mpm. Drawing-annealing-extended annealing experiments were carried out in a continuous operation.

Two zone drawing and annealing

The SAHM draw unit consisting of three pairs of scanted rolls was used for the purposes of two zone drawing studies. Maximum possible draw ratio with satisfactory processing without filament breaks was applied in two zones with majority of the total draw ratio (TDR) being achieved in the first zone at 95°C and remaining part of TDR was applied in the second zone at 100°C. Annealing was carried out using a 1-m long heater that was placed after third draw roll pair. The process was operated at 15 ± 2 mpm.

Fiber characterization

Fiber properties such as denier (g/9000 m length of the fiber), tenacity, elongation, tensile modulus, degree of crystallinity, overall molecular orientation, crystalline and amorphous orientation, crystal size, and long period were characterized. Tensile properties were evaluated using Thwing Albert tensile tester with a gauge length of 25.4 mm. Ten filaments were analyzed from each fiber sample. Crystallinity was determined using differential scanning calorimetry (DSC) and wide angle X-ray scattering (WAXS). Herman's orientation factor for crystalline region was determined from the WAXS pin-hole patterns obtained from parallel arrays of multifilament yarn. Reflections of crystal planes (110) and (200) were used for these calculations. Birefringence was measured using a polarized light optical microscope equipped with 20 order Ehringhaus compensator. Amorphous orientation factor was calculated from crystallinity, birefringence, and crystalline orientation. Details of these characterization techniques were reported in our earlier publications.[1,2]

To determine crystal thickness along the fiber axis, selected fiber samples were analyzed using WAXS for (00l) reflections. The Phillips diffractometer in transmission geometry was used for this study. Based on the crystal structure study of PPS carried out by Tabor et al.,[7] (00l) reflections such as (002), (004), and (006), if present, will occur at 2θ equal to 17.28°, 34.98°, and 53.59°, respectively. CuKα X-rays were used with generator settings at 45 kV and 40 mA. Fixed divergent slit with 1 mm opening was used. The parallel arrays of multifilament yarn were wound on a specimen holder, and the sample holder was set up in such a way that only (00l) reflections will occur from PPS fibers. 2θ scan in the range of 10° to 60° was carried out with 1 s per step. Subsequently, with the help of the X'pert High Score Plus software, the peaks corresponding to (00l) reflections were evaluated for full width at half maximum (FWHM). To consider the effect of instrument broadening, a Si standard was evaluated under the same WAXS geometry.

Surface morphology of a few select fibers was evaluated using the LEO scanning electron microscope (SEM). The draw-annealed fibers were carefully cut longitudinally using a razor blade to reveal internal structure. Gold sputter coating was avoided to reveal the true fiber morphology in SEM at higher magnifications. Since samples were not sputter coated, a lower beam voltage of 1 kV was used to prevent sample charging.

RESULTS AND DISCUSSION

Effect of annealing on structure–properties development

Annealing without drawing

The role of annealing without drawing in enhancing the fiber structure and properties of as-spun fibers is illustrated in Figure 1. The structure of as-spun fiber is not fully developed as indicated by lower molecular orientation and lower degree of crystallinity. At higher take-up speed and lower throughput, even though spinline stresses are high to cause better chain orientation along the fiber axis when compared with the fibers spun at lower take-up speeds, time available for chain orientation, and crystallization is very short due to rapid cooling of finer filaments. Therefore, such as-spun fiber possesses lower tenacity. Upon annealing this fiber at 150°C without any drawing, tenacity increased from 3.5 gpd to 4.5 gpd with breaking elongation decreasing to around 24% [Fig. 1(a)]. Improvement in tensile properties was brought about by morphological improvement, i.e., considerable increase in both,

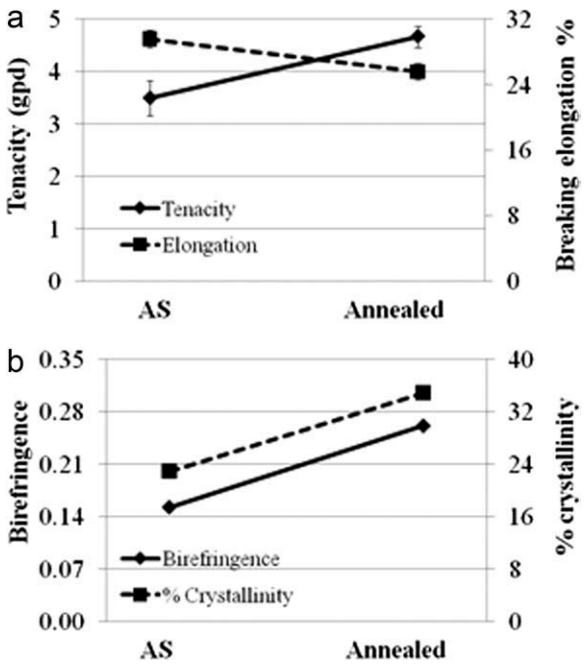

Figure 1 (a) Effect of annealing on tensile properties. (b) Effect of annealing on morphology. (Fiber details: polymer 3P; ET: 315°C; throughput: 9 g/min/12 holes; take-up speed: 2350 mpm; capillary l/d: 10; annealing temperature: 150°C).

overall molecular orientation and crystallinity [Fig. 1(b)]. Considerable increase in birefringence suggests that the stresses developed, due to combination of constant length during annealing and thermally induced chain mobility, and due to attempts by preexisting crystals to grow, growth of which was hindered due to rapid cooling during fiber spinning, cause existing entanglements to disentangle. The disentangled chain network, under the influence of stresses, orients along the fiber axis, creating suitable conditions for further crystallization and additional chain orientation. These simultaneous ongoing processes of crystallization and orientation cause increase in tenacity and decrease in elongation in an annealed fiber.

Annealing with drawing

The as-spun fiber drawn at 95°C was chosen to compare the contribution of annealing toward structure–properties enhancement in the drawn fibers. The results are plotted in Figure 2.

It is seen from Figure 2(a) that annealing increases the drawn fiber tenacity from 4 to 5 gpd at similar level of breaking elongation. The fiber tenacity continues to further improve upon extended annealing. Figure 2(b) shows that birefringence as well as crystallinity is higher in DA fiber when compared with that in only drawn fiber. Degree of crystallinity reaches a plateau in DA fiber with no further increase in D-A-EA fiber. Birefringence increases in D-A-EA fiber over DA fiber. WAXS pin-hole patterns in Figure 3 indicate the improvement of crystalline orientation after each stage of annealing. No change in crystal width was observed (within experimental error) in drawn fibers when compared with as-spun fibers [Fig. 4(a)]. It may suggest that increase in degree of crystallinity in the former may be through formation of newer crystals, probably after the chains in earlier noncrystalline regions orient. Long period was not observed in either of these fibers. Considerable increase in crystal width as well as presence of long period after annealing may suggest that the increase in crystallinity in the case of annealed fibers is due to growth of existing crystals. Enhancement in molecular orientation, crystal perfection, and periodicity in the structure brought in by annealing in drawn fibers explains the increase in tenacity. Continued enhancement of morphological properties upon extended annealing supports further improvement in fiber tenacity. The role of annealing in improving the amorphous orientation can be

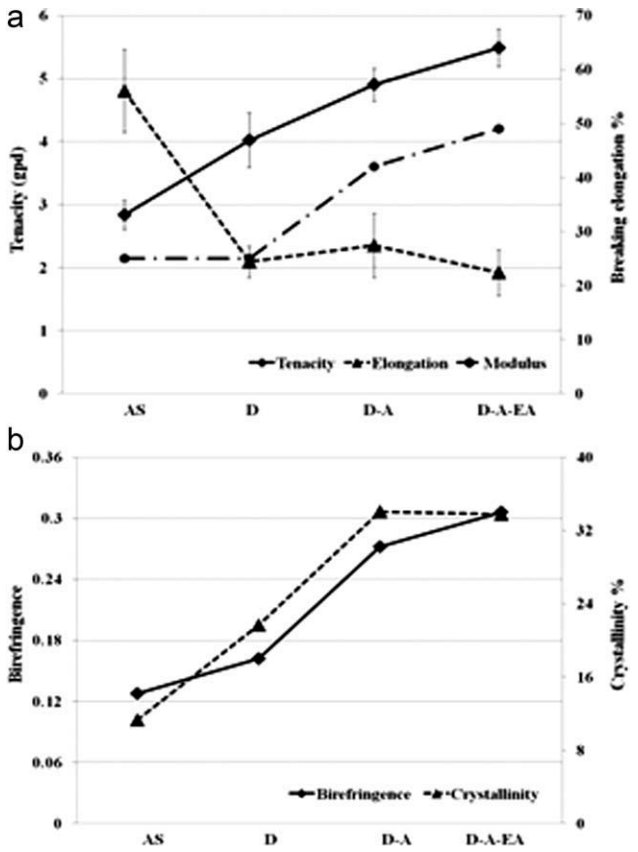

Figure 2 (a) Influence of annealing upon properties enhancement: Tensile properties. (b) Influence of annealing upon properties enhancement: Morphology (Fiber details: polymer 3P; ET: 315°C; throughput: 12 g/min/12 holes; take-up speed: 1750 mpm; capillary l/d: 10; DT: 95°C, annealing temperature: 150°C).

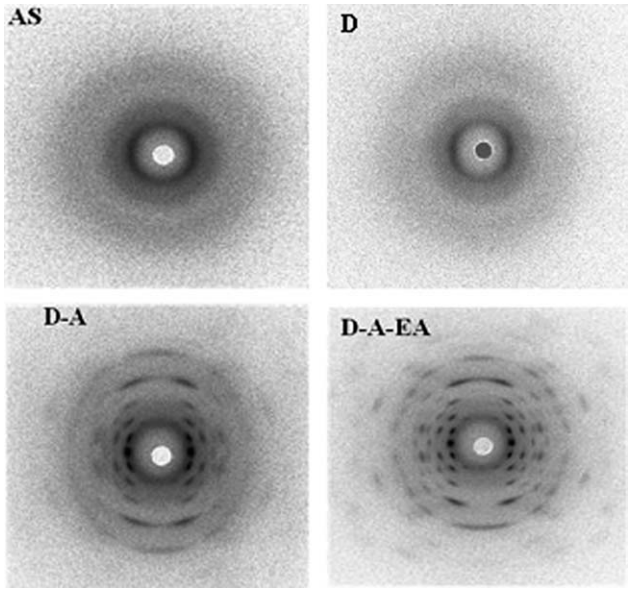

Figure 3 Effect of annealing on crystalline morphology development. (Fiber axis vertical; Fiber details similar as in Fig. 2).

explained as follows. Improvement in long period and crystal growth upon annealing has been reported in other thermoplastic fibers.[8,9] Dismore and Statton[9] proposed the structural model of drawn vis-a-vis annealed fibers. They reported that annealing increases the number of chain folds, and thereby increase the crystal dimensions. In this study, both the orientation factors, f_c and f_{am}, increase [Fig. 4(b)], with comparatively more increase in f_{am}, after annealing when compared with the respective orientation factors in the drawn fibers. Under the influence of constant length annealing, chains in the crystalline region rearrange and the crystals grow, which is in agreement to the observations of earlier investigators.[8,9] Due to these developments, the tie chains may cause chains in the amorphous regions to experience stresses. In the presence of these stresses and the thermal mobility available at annealing temperatures, the chains in the amorphous region orient along the fiber axis. This explains the observed increase in amorphous orientation factors in annealed fibers in comparison with that in drawn fibers. This statement is in agreement to that of Samuels[10] who reported that amorphous orientation increases in isotactic polypropylene fibers possessing f_{am} above certain minimum value, when restrained during heating.

The changes in tensile moduli are plotted for draw annealed fibers in Figure 2(a). In the absence of increase in f_{am} [Fig. 4(b)], tensile modulus remains fairly same in drawn fibers as compared in AS fibers. Considerable improvement in tensile modulus upon annealing and extended annealing can be well correlated with increase in f_{am}.

Two zone drawn and annealed fibers

For the purpose of comparison, 1ZD-A were produced under the same conditions as that of 2ZD-A fibers except the change in number of draw zones. The as-spun fibers that provided highest tenacities after 1ZD-A studies were selected for this investigation. As can be seen from Figure 5, for a given as-spun fiber, drawability is slightly higher when drawn in two zones as compared to when drawn in one zone. It is true for fibers spun from all three polymer types. The reason can be attributed to slower rate of drawing in 2ZD when compared with that in 1ZD.

Tenacity and breaking elongation of 2ZD-A versus 1ZD-A fibers are shown in Figure 6. On tenacity plot, the symbols of equal to and not equal to are the results of mean comparisons obtained using *t*-test. Equal to symbol indicates that the two values are not statistically different, whereas not equal to symbol indicates that the two values are statistically different. Statistically no significant difference is observed between the fiber tenacities obtained by 1ZD-A versus 2ZD-A route in the case of fibers spun from low MW polymers, i.e., 1P and 2P [Fig. 6(a)]. However, in the case of fibers manufactured from high MW polymer (3P), 2ZD-A fibers show significantly higher tenacities [Fig. 6(a)] and lower elongation [Fig. 6(b)] than 1ZD-A fibers. Birefringence and degree of crystallinity do not show significant differences between 1ZD-A and 2ZD-A

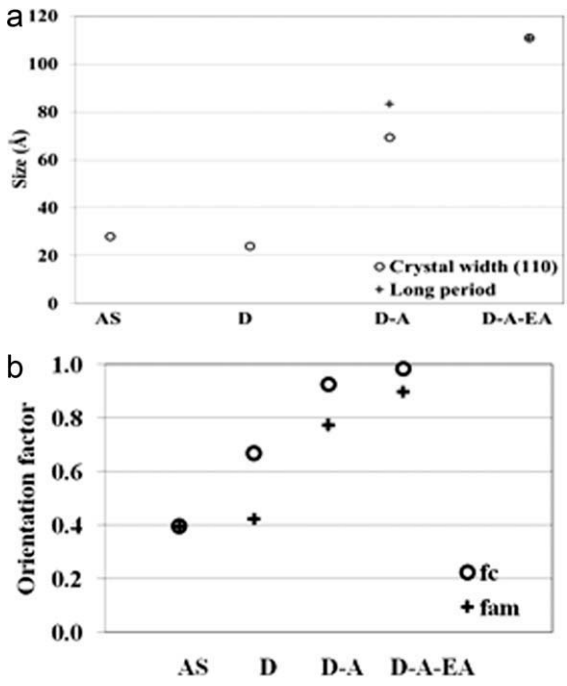

Figure 4 (a) Effect of annealing on crystal dimension. (b) Effect of annealing on orientation factor (Fiber details similar as in Fig. 2).

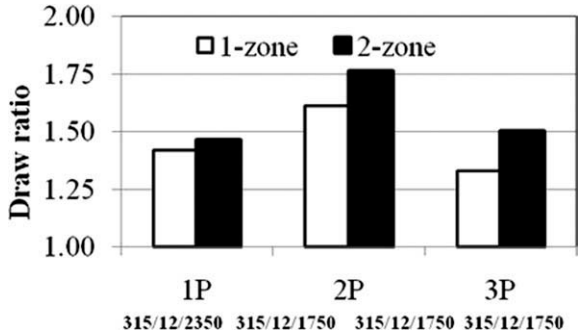

Figure 5 Effect of number of draw zones on drawability (Fiber details: 315/12/2350: extrusion temperature/throughput/take-up speed; capillary l/d: 10; draw temperature: one zone: 95°C; two zone: 95°C/100°C; annealing temperature: 190°C).

fibers [Fig. 6(c,d), respectively]. However, it is to be noted that the crystallinity index determined by WAXS in the case of 3P fibers is found to be higher in 2ZD-A than in 1ZD-A fibers (Table I). These were the only two samples in entire study where discrepancy was observed between degree of crystallinity determined from DSC and WAXS analysis. Figure 7 shows the WAXS pin-hole patterns of 1ZD-A and 2ZD-A fibers, and the morphological properties of these fibers are listed quantitatively in Table I. Some increase is observed in crystal width and long period in 2ZD-A fibers than in 1ZD-A fibers, indicating somewhat larger crystals in 2ZD-A fibers. About

TABLE I
Morphological Properties Comparison between 1ZD-A and 2ZD-A Fibers (Polymer 3P, Other Conditions of Fiber Manufacture Same as in Fig. 6)

Sample	Crystallinity index (WAXS)	f_c	f_{am}	Crystal width (Å) (110)	Long period (Å)
1ZD-A	35	0.964	0.839	77	91
2ZD-A	42	0.957	0.872	91	99

7% increase in X-ray crystallinity with little increase in crystal size may suggest higher taut tie chains fraction in 2ZD-A fibers than in 1ZD-A fibers. As listed in Table I, fairly similar f_c but some increase in f_{am} is seen in the case of 2ZD-A fiber than in 1ZD-A fiber. Therefore, higher fraction of taut tie chains which are oriented better along fiber axis seem to be contributing to considerable increase in fiber tenacity and decrease in breaking elongation.

Structural model in high tenacity PPS fibers

Prevorsek et al.[11] proposed a fibrillar model for nylon-6 and PET fibers. The fibrillar model consists of noncrystalline region between the crystallites along the fiber axis within a microfibril, as well as presence of noncrystalline region between the neighboring microfibrils along the fiber axis. Broader SAXS patterns in present investigation suggest varying size of long periods in PPS fibers. However, the

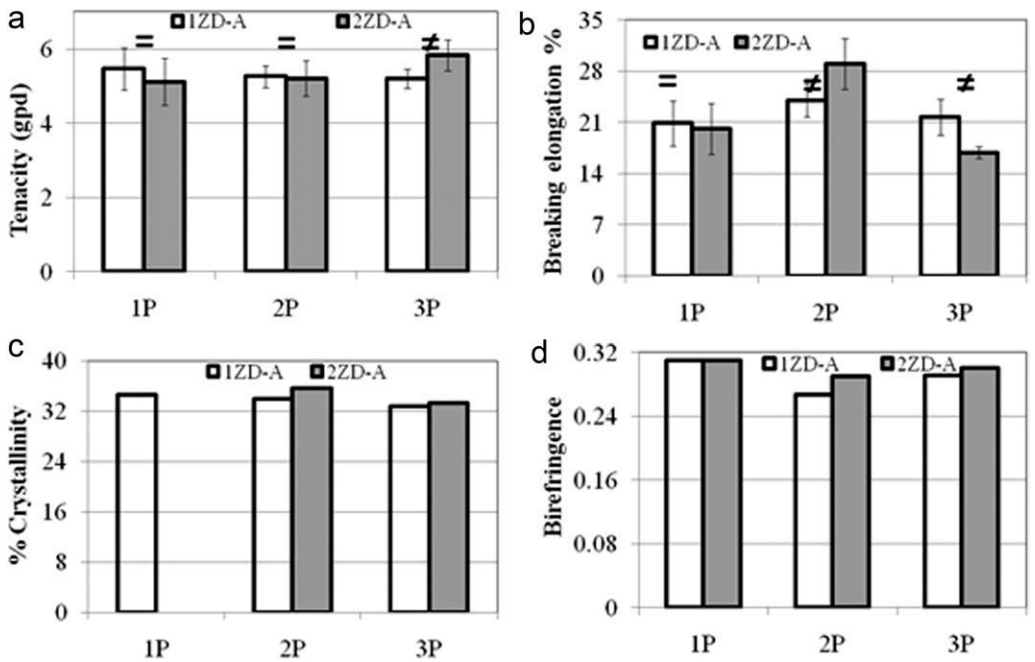

Figure 6 (a) Fiber properties enhancement one zone versus two zone drawing: tenacity. (b) Fiber properties enhancement one zone versus two zone drawing: elongation. (c) Fiber properties enhancement one zone versus two zone drawing: crystallinity. (d) Fiber properties enhancement one zone versus two zone drawing: birefringence (Fiber details: ET: 315°C; throughput: 12 g/min/12 holes; take-up speed: 1P: 2350 mpm; 2P and 3P: 1750 mpm; capillary l/d: 10; DT: 95°C (1Z); 95°C/100°C (2Z), annealing temperature: 190°C).

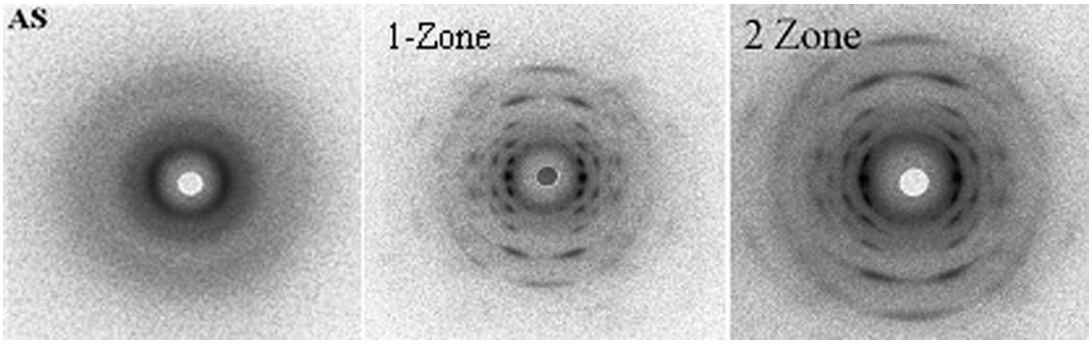

Figure 7 Effect of number of draw zones on crystalline morphology development. (Fiber details: Polymer: 3P; other conditions same as in Fig. 6, Fiber axis vertical).

crystal thickness along the fiber axis determined from (00l) reflections in WAXS studies for some selected DA fibers was found to be more consistent since the reflections corresponding to planes (004) and (006) were narrower. Crystal thickness calculated from (004) reflection for 1ZD-A fiber was found to be 80 Å, whereas the maximum in SAXS pattern corresponds to the long period of 91 Å. After due consideration of variations in long period, it can be fairly stated that noncrystalline region between crystallites along the fiber axis is very small. Periodic lay-up of such crystallites and noncrystalline regions constitutes the microfibrils. Possessing 60–65% noncrystalline region in these high tenacity PPS fibers indicates that the majority of noncrystalline region probably exists between the neighboring microfibrils, similar to the structural model proposed by Prevorsek et al.[11]

SAXS pattern of 2ZD-A fiber manufactured from polymer 3P is shown in Figure 8(a) and corresponding intensity profile is shown in Figure 8(b). Intensity maximum corresponding to the long period in PPS fibers is also indicated in Figure 8(b). Salient points to note from the SAXS pattern are broad and weak intensity on meridian and its absence on equator. Presence of intensity maxima in SAXS pattern suggests the existence of periodicity of crystalline and noncrystalline region along the fiber axis. Intensity corresponding to this maximum is lower, and also, the PPS chains are less flexible when compared with nylon-6 and PET. These points may suggest that unlike the regular chain folding with adjacent reentry proposed by Prevorsek et al.[11] in latter polymers, chain folding in PPS fibers may be more of nonadjacent reentry type. Higher persistence length in a similar polymer, PEEK, around 54 Å[12] when compared with 13 Å in PET[13] may support the difficulties in regular chain folding in semirigid polymer chains like PPS. Marand et al.[14] reported that for stiff polymers like PPS, the adjacent reentry of the chains by folding is unlikely. Based on these arguments, the switchboard model proposed by Flory[15] may be more appropriate for the crystallites in PPS.

The fraction of taut tie chain (β) in the intrafibrillar region can be calculated if E (elastic modulus) and L_{00l}/L is known. It can be estimated using the eq. (1).[16]

$$\beta = E(1 - L_{00l}/L) \Big/ E_c\left(1 - \frac{E(1 - L_{00l}/L)}{E_c}\right) \qquad (1)$$

Above equation assumes that the taut tie chains are distributed uniformly over the cross section of intrafibrillar noncrystalline region. E_c is the elastic modulus of a single crystal. Unwin and Ward[17] have reported a theoretical maximum elastic modulus for PPS to be around 43 GPa.

For one zone drawn and annealed fiber sample for which all required parameters were evaluated (L_{004} = 80 Å, L = 91 Å, E = 49 gpd = 5.93 GPa), the fraction of taut tie chains was found to be 0.0189. To put this value in perspective, Hofmann et al. have reported the fraction of taut tie chains for gel-spun/hot-drawn high-modulus (70 GPa) polyethylene fibers (Spectra 900),[18] and for high modulus (13.4 GPa) poly(ethylene terephthalate) fibers[19] to be around 0.036 and 0.093, respectively. In comparison with these two cases, the fraction is lower in PPS fibers. One of the probable reasons may be lower

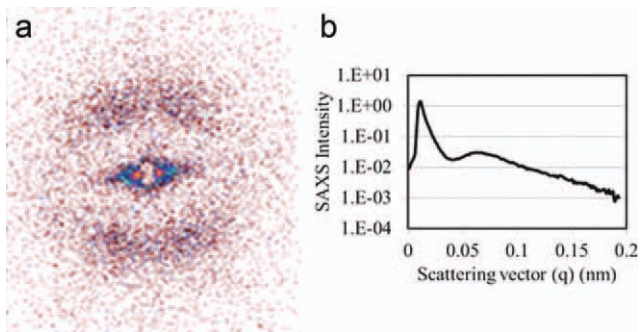

Figure 8 (a) SAXS pattern of 2ZD-A PPS fiber (Fiber axis vertical). (b) SAXS intensity versus scattering vector (Fiber details: Polymer 3P, other processing conditions similar as in Fig. 6). [Color figure can be viewed in the online issue, which is available at wileyonlinelibrary.com.]

MW of PPS used in these studies when compared with PE and PET fibers reported by above researchers. In addition to higher orientation in the noncrystalline region, higher fraction and uniform length distribution of taut tie chains, and higher crystallinity are very much necessary to obtain high modulus fibers.[19] The modulus of PPS fibers in this study was found to be around 50 gpd (~ 6 GPa) which is much lower than its theoretical maximum (~ 43 GPa).[17] Amorphous orientation factor (f_{am}) for this fiber was found to be 0.839 which is fairly high. Therefore, lower modulus suggests that, besides lower fraction of taut-tie chains, the length distribution of the intrafibrillar tie-chains may not be uniform. Broad and weak intensity in SAXS pattern suggests variations in long period. Fairly uniform crystal thickness (sharp WAXS reflections from 00l planes) may suggest that variations in long period originate from varying lengths of intrafibrillar noncrystalline region. It supports higher probability of nonuniform length distribution of intrafibrillar taut-tie chains. It is discussed earlier that the majority of the noncrystalline region exists in the interfibrillar region. It implies that the intrafibrillar noncrystalline region is smaller in length. Under these circumstances, the probability of out-of directional dimension in the intrafibrillar tie-chain region may be low.

Absence of equatorial reflection in SAXS pattern in PPS fibers suggests that there is no detectable periodicity perpendicular to the fiber axis. The arc-type meridional reflection in SAXS patterns suggests that the crystallites in adjacent microfibrils are in a skewed arrangement, skewness of which may be higher than the one proposed by Prevorsek et al.[11] in PET fibers based on four point pattern.

Based on above discussion, highly oriented chains along the fiber axis in noncrystalline region, and the presence of taut tie-chains as envisaged to explain

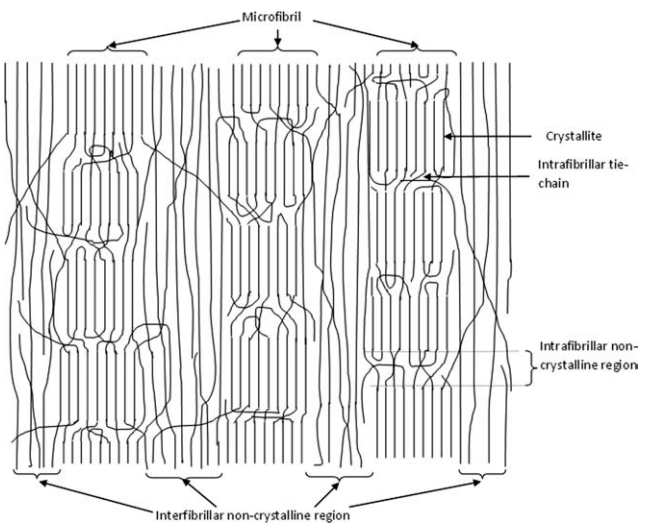

Figure 9 Proposed structural model for high tenacity PPS fibers.

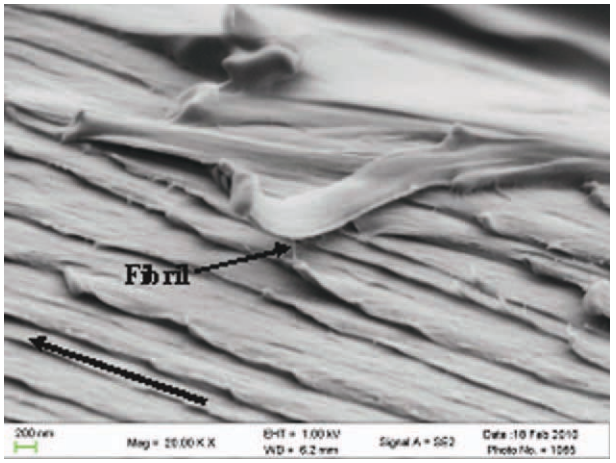

Figure 10 SEM micrograph of two zone draw-annealed fiber. (Arrow in lower left corner indicates fiber axis), (Polymer 3P, spun at 1750 mpm, ET: 315°C, capillary l/d: 10; Throughput: 12 g/min/12 holes, DT: 95°C/100°C, AT: 190°C). [Color figure can be viewed in the online issue, which is available at wileyonlinelibrary.com.]

the tensile properties, the probable structural model in high tenacity PPS fibers is depicted in Figure 9.

SEM micrograph shown in Figure 10 is taken of fiber having tenacity, ca. 6 gpd after slicing it longitudinally using razor blade. It is to be noted that due to the difficulties involved in careful peeling of cut section, observation was performed on a sliced surface unlike of a peeled surface as reported by other investigators while studying fiber morphology by SEM.[20–22] On a macroscopic view, it appears that the cut surface (upper right hand corner of the image) resulted in tearing-off the fiber at remaining portion (lower part of the image). Presence of multilayer structure is evident perpendicular to fiber axis. Careful observation of the surface of each layer exhibits fibrillar structure in it. One such fibril connecting adjacent layers is also indicated, and fibrils are distinguishably evident at a few other places. The dimension of this fibril is around 200 Å and may be comprising of very few microfibrils since crystal width reported in this fiber is around 90 Å (based on (110) reflection) and around 60 Å (based on (200) reflection). Thus presence of fibrillar structure as proposed in the structural model (Fig. 9) is supported by the SEM micrographs. Thickness of each layer appears to be equal to a few hundred angstroms.

CONCLUSIONS

It was shown that as-spun fibers with very little drawability can be annealed to provide PPS fibers with fairly good level of tenacity (~ 4.5 gpd) with acceptable level of elongations (20–25%). Annealing and extended annealing helped in improving fiber properties of drawn fibers by increasing crystallinity,

crystal perfection, and molecular orientation in crystalline as well as noncrystalline regions. Under optimum drawing conditions, two zone draw-annealed fibers manufactured from high MW polymer, 3P showed highest tenacities, to the level of around 6 gpd with 20% breaking elongation. Probable structural model in high tenacity PPS fibers was proposed based on numerous studies of tensile and morphological properties.

The authors sincerely thank Ticona Polymers, a business of Celanese Chemicals, for funding this research project and for supplying various grades of proprietary Fortron® PPS polymers used. Continued interaction with Dr. Manoj Ajbani, Dr. Ke Feng, and Lisa baker (all from Ticona Polymers) is gratefully acknowledged.

References

1. Gulgunje, P. V.; Bhat, G. S.; Spruiell, J. E. J Appl Polym Sci, 2011, 122, 3110.
2. Gulgunje, P. V.; Bhat, G. S.; Spruiell, J. E. J Appl Polym Sci, to appear.
3. Wang, L. C.; Dobb, M. G.; Tomka, J. G. J Text Inst 1995, 86, 395.
4. Ahmed, M. Polypropylene Fibers, Science and Technology; Elsevier Science Publishing Co.: Amsterdam, 1982; p 389.
5. Suzuki, A.; Kohno, T.; Kunugi, T. J Polym Sci Part B: Polym Phys 1998, 36, 1731.
6. Krins, B.; Feijen, H. H. W.; Heuzeveldt, P.; Vieth, C. R. E. Diolen Industrial Fibers Bv Netherlands Canadian Patent 2,601,751 (2006).
7. Tabor, B. J.; Magre, E. P.; Boon, J. Eur Polym J 1971, 7, 1129.
8. Gupta, V. B.; Kumar, S. J Appl Polym Sci 1981, 26, 1897.
9. Dismore, P. F.; Statton, W. O. J Polym Sci 1966, C13, 133.
10. Samuels, R. J. J Polym Sci Part B: Polym Phys 1975, 13, 1417.
11. Prevorsek, D. C.; Kwon, Y. D.; Sharma, R. K. J Mater Sci 1977, 12, 2310.
12. Bishop, M.; Karasz, F.; Russo, P.; Langley, K. Macromolecules 1985, 18, 86.
13. Imai, M.; Kaji, K.; Kanaya, T.; Sakai, Y. Phys Rev B 1995, 52, 12696.
14. Marand, H.; Xu, J.; Srinivas, S. Macromolecules 1998, 31, 8219.
15. Flory, P. J. J Am Chem Soc 1962, 84, 2857.
16. Peterlin, A. In Ultra High Modulus Polymers; Ciferi, A., Ward, I. M., Eds.; Applied Science: London, 1979.
17. Unwin, A. P.; Ward, I. M. Polym Commun 1988, v20, 520.
18. Hofmann, D.; Schulz, E. Polymer 1989, v30, 1964.
19. Hofmann, D.; Göschel, U.; Walenta, E.; Geiß, D.; Philipp, B. Polymer 1989, v30, 242.
20. Scott, R. G. ASTM Bull 1959, 257, 121.
21. Val Veld, R. D.; Morris, G.; Billica, H. R. J Appl Polym Sci 1968, 12, 2709.
22. Bodaghi, H.; Spruiell, J. Int Polym Process 1988, 3, 100.